

---

# Extending Graph Condensation to Multi-Label Datasets: A Benchmark Study

**Liangliang Zhang**  
*Rensselaer Polytechnic Institute*

*zhangl41@rpi.edu*

**Haoran Bao**  
*Rensselaer Polytechnic Institute*

*baoh2@rpi.edu*

**Yao Ma**  
*Rensselaer Polytechnic Institute*

*may13@rpi.edu*

## Abstract

As graph data grows increasingly complicate, training graph neural networks (GNNs) on large-scale datasets presents significant challenges, including computational resource constraints, data redundancy, and transmission inefficiencies. While existing graph condensation techniques have shown promise in addressing these issues, they are predominantly designed for single-label datasets, where each node is associated with a single class label. However, many real-world applications, such as social network analysis and bioinformatics, involve multi-label graph datasets, where one node can have various related labels. To deal with this problem, we extends traditional graph condensation approaches to accommodate multi-label datasets by introducing modifications to synthetic dataset initialization and condensing optimization. Through experiments on eight real-world multi-label graph datasets, we prove the effectiveness of our method. In experiment, the GCond framework, combined with K-Center initialization and binary cross-entropy loss (BCELoss), achieves best performance in general. This benchmark for multi-label graph condensation not only enhances the scalability and efficiency of GNNs for multi-label graph data, but also offering substantial benefits for diverse real-world applications.

## 1 Introduction

Graph-structured data are fundamental to many real-world applications, including social networks, academic citation networks, chemical molecules, protein-protein interaction networks, mapping services, and product recommendation systems Battaglia et al. (2018); Wu et al. (2020); Zhou et al. (2020); Wu et al. (2022). In these graph structures, nodes represent entities (e.g., users in social networks), while edges represent relationships between these entities (e.g., social connections between users)Zhang et al. (2023).

Graph Neural Networks (GNNs) are a class of deep learning models specifically designed to process and learn from graph-structured data. It utilizes the topology of the graph to capture dependencies and learn meaningful nodes, edges, and graph-level representations. By extending deep learning to non-Euclidean domains, GNNs have achieved state-of-the-arts performance in many graph machine learning applications Zhang et al. (2023); Hamilton et al. (2018). For example, in the recommendation system Li et al. (2019); Mao et al. (2021); Wu et al. (2022); Zhang et al. (2019a), drug discoveries Jiang et al. (2021); Duvenaud et al. (2015); Zhang et al. (2021), fraud account detection Dou et al. (2020); Wang et al. (2021) and traffic forecasting Jiang & Luo (2022). GNNs combine the node features and structure of graph as the input and output the representations of graph information Hamilton et al. (2018); Velickovic et al. (2017); Kipf & Welling (2016). Among all the GNNs techniques, the most broadly followed methods is recursive neighborhood aggregation scheme, which aims to get the representation of each node, respectively Xu et al. (2018). By applying different neighborhood aggregation and graph-level pooling methods, GNNs are capable of handling

---

various of tasks like node classification Xiao et al. (2022), link prediction Hasan & Zaki (2011), and graph classification Zhang et al. (2018).

Even though GNNsZhang et al. (2023; 2019b) are widely used for analyzing graphs, training these models on large-scale graphs is still computationally expensive Gao et al. (2018); Bojchevski et al. (2020). Furthermore, nowadays, graph data is becoming gigantic with numerous nodes and edges in a single graph Zhang et al. (2023). For example, the Twitter user graph has 288M monthly active users as of 3/2015 and an estimated average of 208 followers per user for an estimated total of 60B followers (edges) Ching et al. (2015). Such industry graphs can be two orders of magnitude larger, like hundreds of billions or up to one trillion edges. In other words, the complexity and large scale of graph data pose significant challenges for training GNNsJin et al. (2022b). Despite the scalability challenges, for some specific applications that need re-training multiple times models would encounter more hardships rather than computation cost.

To address these large-scale datasets challenges, graph condensation methods recently Xu et al. (2024); Gao et al. (2024) have gained lots of attention. Graph condensation is motivated by condensing a large graph dataset into a smaller informative synthetic graph, thereby enhancing the scalability and efficiency of GNNs Xu et al. (2024); Gao et al. (2024); Hashemi et al. (2024). The goal is to achieve comparable performance in GNNs using this synthetic small graph, instead of relying on the original large-scale graph Loukas (2018); Jin et al. (2022a). By doing so, condensed synthetic graph enables GNNs to maintain strong predictive performance while significantly reducing the computational resources required for tasks such as training and inference. By eliminating redundant information in original dataset, it makes the synthetic graph more manageable within the constraints of limited computation resources, thereby providing better support for graph data mining tasks and applications such as Continual learning Liu et al. (2023), Network Architecture Search (NAS)Gao et al. (2021), etc. Moreover, take node classification task as an example, the node can be well classified is because GNNs have learned to capture the unique pattern of nodes to distinguish them from other nodes in different classes.

Existing graph condensation works Xu et al. (2024); Gao et al. (2024) investigate different condensing strategies including gradient distance matchingJin et al. (2022b); Yang et al. (2023), trajectory matchingZheng et al. (2024); Zhang et al. (2024), kernel ridge regressionXu et al. (2023); Wang et al. (2024), and distribution matchingLiu et al. (2022; 2023). Even though they have achieved great success, the original and synthetic datasets are all single-label ones. In many real-world scenarios, the nodes of graph can be associated with multiple labels in lots of situations Huang & Zhou (2012); Read et al. (2011). For instance, users are allowed to join multiple groups that respectively represent their diverse interests. Therefore, nodes of social networks Shi et al. (2019) are annotated with several tags profiling users’ preferences in different domains. Similarly, a paper in a citation network Akujuobi et al. (2019) may be associated with multiple research topics, and in the protein-protein interaction networks Zeng et al. (2019), it is used to classify protein functions in biology, which are associated with multiple biological processes, like molecular activities or cellular components. These functions are typically inferred based on how proteins interact with one another, with each interaction providing insight into the role of protein within the cell, such as catalyzing reactions, transporting molecules, or transmitting signals. So in the application of graph datasets, multi-label node classification is a fundamental and practical task in graph data miningShi et al. (2019; 2020); Akujuobi et al. (2019); Zhao et al. (2023). In the multi-label graph scenario, each node not only has content (or features) but also associated with multiple class labels. The goal is to assign one or more labels to each node. However, existing graph condensation techniques are designed to address the single-label graph scalability issue, typically condensing the large graph based on class-wise condensing. In this way, it can be hard for us to get the synthetic small graph from the multi-label graph datasets. While directly applying single-label condensation methods to multi-label graphs would result in a loss of critical information, as the class-wise assumption does not hold. This reminds as the open challenge.

To bridge this gap from single-label to multi-label setting, in this work, we adapt available graph condensation techniques to the mainstream multi-label datasets. Our approach includes modifications to the synthetic dataset initialization and original datasets condensation matching stages. By evaluating various adaptation settings, we identify three key insights into the optimal combination of initialization and optimization methods. Using these best settings, we further analyze graph condensation models and present three additional observations, highlighting the unique challenges of condensing multi-label graph datasets.

---

Our contributions are as follows:

1. We extend classic SOTA graph condensation methods, including GCond, GCDM, and SGDD, to the multi-label graph dataset scenario by introducing multi-label synthetic dataset initialization and condensing optimization methods.
2. To find the best adaption strategies, we compare different initialization techniques such as Random sampling, Herding, K-Center and probability synthetic multi-label combine with two different multi-label loss functions – SoftMarginLoss and BCELoss.
3. With the best adaption settings, we evaluate the condensation methods with F1-micro and F1-macro scores on eight real-world multi-label datasets: PPI, PPI-large, Yelp, DBLP, PCG, HumanGo, EukaryoteGo, and OGBN-Proteins. Finally, we find the GCond method generally works best with K-Center initialization and BCELoss.

## 2 Related Work

### 2.1 Graph Neural Networks

Graph Neural Networks (GNNs) are a class of deep learning models specifically designed to process and learn from graph-structured data. GNNs have achieved outstanding performance in many graph machine learning applications Zhang et al. (2023); Hamilton et al. (2018). For instance, in the recommendation system on social network Li et al. (2019); Mao et al. (2021); Wu et al. (2022); Zhang et al. (2019a), drug discoveries from molecule graphs Jiang et al. (2021); Duvenaud et al. (2015); Zhang et al. (2021), fraud account detection on financial graphs Dou et al. (2020); Wang et al. (2021) and traffic forecasting in transportation graph Jiang & Luo (2022).

GNNs combine the node features and structure of graph as the input and output the representations of graph Hamilton et al. (2018); Velickovic et al. (2017); Kipf & Welling (2016). Among all the GNNs techniques, they broadly follow a recursive neighborhood aggregation scheme to get the representation of each node Xu et al. (2018). Some of the typical GNNs models like the Graph Convolutional Network (GCN) Kipf & Welling (2016) operate by aggregating and transforming information from neighboring nodes layer by layer. Variants like Graph Attention Networks (GAT) Velickovic et al. (2017) use attention mechanisms to prioritize certain neighbors, while GraphSAGE Hamilton et al. (2017) samples neighborhoods to scale to large graphs. By applying different neighborhood aggregation and graph-level pooling methods, GNNs are capable of handling various of tasks Xiao et al. (2022); Hasan & Zaki (2011); Zhang et al. (2018) like node classification, link prediction, and graph classification.

### 2.2 Multi-Label Classification on Graphs

Multi-label classification on graphs is a fundamental task in graph machine learning, where nodes in a graph are associated with multiple labels simultaneously. This task is critical in numerous real-world applications, including social networks, bioinformatics, and recommendation systems. For instance, in social networks, users may belong to multiple interest groups, while in bioinformatics, proteins may participate in multiple biological processes such as molecular functions and cellular activities Huang & Zhou (2012); Read et al. (2011); Shi et al. (2019); Akujuobi et al. (2019). In multi-label classification, the goal is to predict a set of labels for each data point in the dataset. The labels can be thought of as binary variables, where a label is either present (1) or absent (0). Recently, there have been several approaches that use neural networks for multi-label classification.

Traditional multi-label classification methods relied on adapting single-label classification techniques to multi-label scenarios. Popular strategies include problem transformation methods (e.g., binary relevance and classifier chains) and algorithm adaptation approaches, which extend existing classifiers to handle multiple labels directly Read et al. (2011); Tsoumakas & Katakis (2008). These approaches use architectures such as recurrent neural networks (RNNs) and convolutional neural networks (CNNs) to learn representations of the

input data and make predictions for the labels. However, these approaches were not designed to exploit the graph structure and are therefore suboptimal for graph data.

With the advent of GNNs, researchers began exploring multi-label classification directly on graph-structured data. GNNs excel in capturing the relational and topological information of graphs, making them well-suited for multi-label classification tasks. For example, GraphSAGE Hamilton et al. (2017) and GAT Velickovic et al. (2017) utilize neighborhood aggregation to generate node embeddings, which can be fed into multi-label classifiers. Specialized models like ML-GCN Chen et al. (2019) integrate graph convolutional layers with multi-label prediction heads to improve performance on multi-label datasets.

### 2.3 Graph Condensation

Despite the impressive performance of GNN models, training them on large-scale datasets is often challenging due to high computational costs, especially when retraining or dealing with redundant information. To address these issues, graph condensation techniques have been developed. These methods distill a large-scale graph into a smaller yet informative synthetic graph, improving the scalability and efficiency of GNNs Xu et al. (2024); Gao et al. (2024); Hashemi et al. (2024). The condensation process generates a compact representation that preserves essential topological and feature-based properties from the original graph Loukas (2018); Jin et al. (2022a). This allows GNNs to achieve comparable performance using the condensed graph while significantly reducing the computational resources needed for training and inference.

Existing graph condensation works Xu et al. (2024); Gao et al. (2024) investigate different condensing strategies including gradient distance matching Jin et al. (2022b); Yang et al. (2023), trajectory matching Zheng et al. (2024); Zhang et al. (2024), kernel ridge regression Xu et al. (2023); Wang et al. (2024), and distribution matching Liu et al. (2022; 2023). Condensed graphs facilitate more efficient model execution without sacrificing the quality of learning, making this technique a promising method for real-world GNN deployments. By eliminating redundant information in original dataset, graph condensation makes the synthetic graph more manageable within the constraints of limited computation resources, thereby providing better support for graph data mining tasks and applications such as Continual learning Liu et al. (2023) and Network Architecture Search (NAS) Gao et al. (2021), etc. Moreover, take node classification as an example, the reason a node can be well classified is that GNNs have learned to capture the unique pattern of nodes to distinguish them from other nodes in different classes.

## 3 Problem Formulation

Consider a graph  $\mathcal{G} = \{A, X, Y\}$ , where  $N$  is the number of nodes,  $A \in \mathbb{R}^{N \times N}$  is the corresponding adjacency matrix,  $X = \{x_1, x_2, \dots, x_N\} \in \mathbb{R}^{N \times d}$  is the  $d$ -dimensional node feature matrix. In multi-label scenario, each node is associated with multiple labels revealing characteristics or semantics of the node. In this case, the label matrix can be represented as  $Y \in \{y_1, y_2, \dots, y_N\} \in \{0, 1\}^{N \times K}$ , where  $K$  is the number of classes. Following the definition of graph condensation, our goal is to learn a smaller synthetic graph denoted as  $\mathcal{S}$ , which can contain the ability to train downstream tasks' GNNs and achieve competitive performance compared with the original large-scale complex graph  $\mathcal{G}$ . Similarly, the synthetic graph can be denoted as  $\mathcal{S} = \{A', X', Y'\}$  along with  $A' \in \mathbb{R}^{N' \times N'}$ , and  $X' \in \mathbb{R}^{N' \times d}$ ,  $Y' \in \{0, 1\}^{N' \times K}$ . During this stage, our expectation is that the scale of the synthetic graph can be much smaller compared with the original graph, denotes as  $N' \ll N$ .

In this work, we adapt the graph condensation techniques to a multi-label setting, trying to get the synthetic multi-label graph. First, we introduce the general framework of graph condensation in Figure 1. Generally, graph condensation methods are using different matching strategies to optimize the synthetic graph  $\mathcal{S}$  similar to the original graph  $\mathcal{G}$ . Despite these various strategies, the key point is to keep the comparable performance of GNNs while training on small graph. Therefore, our objective can be formulated as follows Jin et al. (2022b):

$$\mathcal{S}^* = \arg \min_{\mathcal{S}} \mathcal{M}(\theta_{\mathcal{S}}^*, \theta_{\mathcal{G}}^*) \quad \text{s.t.} \quad \theta^* = \arg \min_{\theta} \mathcal{L}(GNN_{\theta}), \quad (1)$$

where  $GNN_{\theta}$  denotes a GNN parameterized with  $\theta$ . Specifically,  $\theta_{\mathcal{S}}$  and  $\theta_{\mathcal{G}}$  are the parameters trained on graph  $\mathcal{S}$  and  $\mathcal{G}$ , respectively.  $\mathcal{M}(\cdot)$  is the matching strategy used to match the model  $\theta_{\mathcal{S}}^*$  trained synthetic

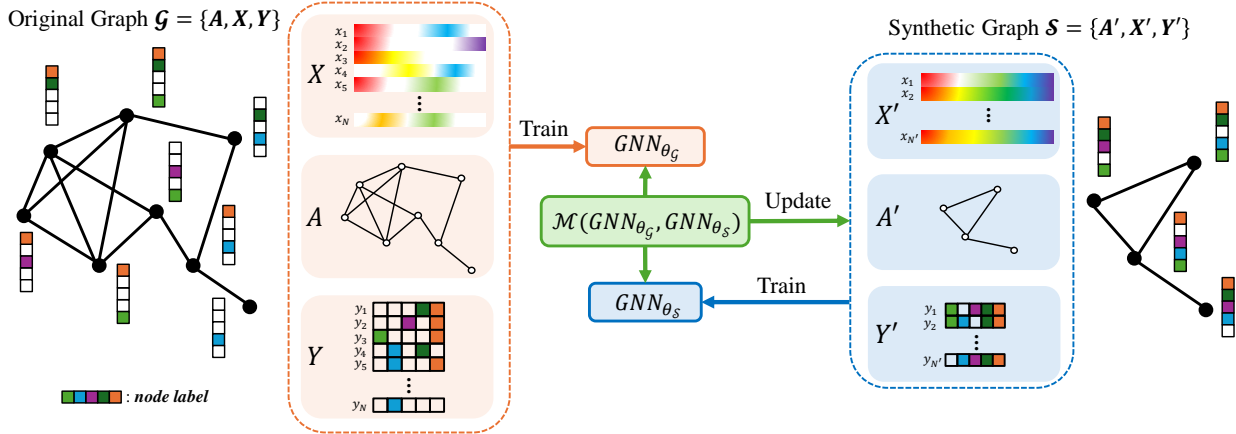


Figure 1: Workflow for multi-label graph condensation. It shows the process of condensing a large multi-label graph  $\mathcal{G} = \{A, X, Y\}$  into a smaller synthetic graph  $\mathcal{S} = \{A', X', Y'\}$ , where  $Y$  and  $Y'$  represent the multi-label matrix. Various matching strategies, denoted by  $\mathcal{M}(\cdot)$ , are employed to ensure that key information in the original graph is captured. Our goal is to use the synthetic graph  $\mathcal{S}$  to train a GNN that achieves comparable performance to the one trained on the original graph  $\mathcal{G}$ , thus reducing graph size while retaining performance.

graph  $\mathcal{S}$  to the one  $\theta_{\mathcal{G}}^*$  trained on the original graph  $\mathcal{G}$ .  $\mathcal{L}(\cdot)$  is the loss function used to measure the difference between model predictions and ground truth. For most graph condensation methods, the loss function is cross-entropy loss.

As the specific initialization of model parameters  $\theta$  can lead to the overfitting problem Jin et al. (2022b), one common solution Wang et al. (2018) is to generate the synthetic data following a distribution of random initializations of  $P_{\theta_0}$ . Furthermore, the reformulated optimization problem as follows:

$$\begin{aligned} \mathcal{S}^* &= \arg \min_{\mathcal{S}} \mathbb{E}_{\theta_0 \sim P_{\theta_0}} [\mathcal{M}(\theta_{\mathcal{S}}^*, \theta_{\mathcal{G}}^*)] \\ \text{s.t. } \theta^* &= \arg \min_{\theta(\theta_0)} \mathcal{L}(GNN_{\theta}). \end{aligned} \quad (2)$$

where  $\theta(\theta_0)$  indicates  $\theta$  is a function acting on  $\theta_0$ .

## 4 Graph Condensation Methods

Building on the global understanding of existing single-label graph condensation methods, we observe that while different graph condensation methods differ primarily in their matching strategies, the overall workflow remains largely consistent. Therefore, before adapting these methods to the multi-label scenario, we will illustrate the different matching strategies of condensation methods first.

### 4.1 GCond: Gradient Matching

By computing the gradient of  $\mathcal{L}$  w.r.t.  $\mathcal{S}$  and optimize  $\mathcal{S}$  via gradient descent. For each training step, the  $opt_{\theta}$  is the update rule, consider the one-step gradient descent for model parameters:

$$\begin{aligned} \theta_{t+1}^{\mathcal{S}} &\leftarrow \theta_t^{\mathcal{S}} - \eta \nabla_{\theta} \mathcal{L}(GNN_{\theta_t^{\mathcal{S}}}(A', X'), Y') \\ \theta_{t+1}^{\mathcal{G}} &\leftarrow \theta_t^{\mathcal{G}} - \eta \nabla_{\theta} \mathcal{L}(GNN_{\theta_t^{\mathcal{G}}}(A, X), Y) \end{aligned} \quad (3)$$

where  $\theta_t^{\mathcal{S}}$  and  $\theta_t^{\mathcal{G}}$  denote the model parameters trained on  $\mathcal{S}$  and  $\mathcal{G}$  at step  $t$ .  $\eta$  is the learning rate for the gradient descent.

By matching the training gradient trajectory, define distance function  $D(\cdot, \cdot)$ , define the gradient matching strategy  $\mathcal{M}_{GCond}$  as:

$$\mathcal{M}_{GCond} = D(\nabla_{\theta}\mathcal{L}(GNN_{\theta_t^S}(A', X'), Y'), \nabla_{\theta}\mathcal{L}(GNN_{\theta_t^G}(A, X), Y)) \quad (4)$$

Assume  $T$  is the number of steps of the whole training, the final optimized objective is:

$$\mathcal{S}^* = \arg \min_{\mathcal{S}} \mathbb{E}_{\theta_0 \sim P_{\theta_0}} \left[ \sum_{t=0}^{T-1} D(\nabla_{\theta}\mathcal{L}(GNN_{\theta_t^S}(A', X'), Y'), \nabla_{\theta}\mathcal{L}(GNN_{\theta_t^G}(A, X), Y)) \right]. \quad (5)$$

Direct joint learning can be highly challenging because the three variables  $A'$ ,  $X'$ , and  $Y'$  in synthetic graph are interdependent. One straightforward way is to treat  $A'$  and  $X'$  as free parameters. By modeling the synthetic graph structure as a function of the condensed node features, synthetic graph structure  $A'$  can be learned by:

$$A' = g_{\phi}(X') \quad (6)$$

where  $\phi$  is the parameter of a multi-layer neural network. So the rewrite objective is:

$$\mathcal{S}^* = \arg \min_{X', \phi} \mathbb{E}_{\theta_0 \sim P_{\theta_0}} \left[ \sum_{t=0}^{T-1} D(\nabla_{\theta}\mathcal{L}(GNN_{\theta_t^S}(g_{\phi}(X'), X'), Y'), \nabla_{\theta}\mathcal{L}(GNN_{\theta_t^G}(A, X), Y)) \right] \quad (7)$$

## 4.2 SGDD: Structure-broadcasting

Instead of treating  $A'$  and  $X'$  in the synthetic graph  $\mathcal{S}$  as free parameters, recent work Yang et al. (2023) points out that this way ignores the original structure  $A$  in  $\mathcal{G}$ . To address this problem, they broadcast  $A$  as supervision for the generation of  $A'$ . By introducing graphon Gao & Caines (2019); Ruiz et al. (2020); Xia et al. (2023) to matching the different shapes between  $A$  and  $A'$ , SGDD use random noise  $\mathcal{Z}(N') \in \mathbb{R}^{N' \times N'}$  as input coordinates. Through the generative model to synthesize an adjacency matrix  $A'$  with  $N'$  nodes, the process can be formulated as:

$$A' = GEN(\mathcal{Z}(N'); \Phi) \quad (8)$$

where  $GEN(\cdot)$  is the generative model with parameter  $\Phi$ . Then the structure optimization is:

$$\mathcal{M}_{structure} = Dis(A, GEN(\mathcal{Z}(N'); \Phi)), \quad (9)$$

where  $A$  is supervision and  $Dis(\cdot)$  is a metric that measure the difference between  $A$  and  $A'$ . By adding the corresponding nodes information from  $X'$  and  $Y'$  to the inherent relation learning Pfeiffer III et al. (2014); Shalizi & Thomas (2011), the revised generation model is  $GEN(\mathcal{Z}(N') \oplus X' \oplus Y'; \Phi)$ ,  $\oplus$  denotes the concatenate operation. In general, SGDD concurrently optimizes the parameters  $X'$  and  $A'$ . While the refinement of  $X'$  is achieved through a gradient matching strategy, whereas the  $A'$  is enhanced using the Laplacian energy distribution(LED) matching technique Tang et al. (2022); Das et al. (2016); Gutman & Zhou (2006). During each step, the other component is frozen to ensure effective refinement, and the overall training loss function can be summarized as:

$$\mathcal{M}_{SGDD} = \mathcal{M}_{GCond} + \alpha \mathcal{M}_{structure} + \beta \|A\|_2, \quad (10)$$

where  $\|A\|_2$  is proposed as a sparsity regularization term,  $\alpha$  and  $\beta$  are trade-off parameters.

## 4.3 GCDM: Distribution Matching

Inspired by the distribution matching strategy in image dataset condensation Zhao & Bilen (2023), GCDMLiu et al. (2022) adapt the receptive field distribution matching method in GNN. In the graph dataset, with the

reproducing kernel Hilbert space  $\mathcal{H}$  defined by GNNs and with in each class  $c$ , GCDM optimize the maximum mean discrepancy (MMD). Let  $\Phi_\theta$  be an  $L$ -layer GNN model parameterized by  $\theta$ , the loss of GCDM is:

$$\mathcal{M}_{GCDM} = \min_{\phi, X'} \sum_{c=0}^{C-1} r_c \cdot \max_{\theta_c} \left\| \frac{1}{V_c} \sum_{i \in V_c} \text{emb}_i^c - \frac{1}{V'_c} \sum_{j \in V'_c} \text{emb}_j^c \right\|_2^2, \quad (11)$$

where the node embeddings are:

$$\{\text{emb}_i^c\}_{i=0}^{N-1} \leftarrow \Phi_{\theta_c}(A, X) \quad (12)$$

$$\{\text{emb}_j^c\}_{j=0}^{N'-1} \leftarrow \Phi_{\theta_c}(A' = g_\phi(X'), X') \quad (13)$$

$V_c$  and  $V'_c$  represent the node sets belong to the class  $c$  of original graph  $\mathcal{G}$  and synthetic graph  $\mathcal{S}$ , respectively.  $r_c$  denotes the condensed class ratio for each class of the synthetic graph.

## 5 Datasets and Experiment Settings

In this section, we first present the multi-label graph datasets used in our benchmark investigation, accompanied by the detailed introduction of label information in real-world application. Next, we detail the evaluation metrics used to assess the effectiveness of the adaptation methods, providing a robust framework for performance comparison.

**Datasets.** Specifically, we employ eight real-world datasets including PPI, PPI-large, Yelp, DBLP, OGBN-Proteins, PCG, HumanGo, EukaryoteGo. The details of those datasets are introduced as follows:

- PPI Zeng et al. (2019) is the Protein-Protein Interaction network. It classifies protein functions based on the interactions of human tissue proteins. Positional gene sets are used, motif gene sets and immunological signatures as features and gene ontology sets as labels (121 in total), collected from the Molecular Signatures Database Liberzon et al. (2015). And PPI-large is the larger version of PPI dataset.
- Yelp Zeng et al. (2019) is processed from a public open dataset from yelp.com. The nodes represent active users and the edges are the relationship between the users. The multi-label of each node represents the types of business like Coffee & Tea, Flowers & Gifts, Tours, and so on. Node features contain the information of all the reviews and rates by users, generated by pre-trained Word2Vec model Church (2017).
- DBLP Akujubi et al. (2019) is the citation network extracted from DBLP. The nodes represent authors and edges are the co-authorship between the authors. Multi-label here indicates the four research areas like database, data mining, information and retrieval and artificial intelligence.
- OGBN-Proteins from Open Graph Benchmark Hu et al. (2020) is an undirected, weighted, and typed (according to species) graph. Nodes represent proteins, and edges indicate different types of biologically meaningful associations between proteins, e.g., physical interactions, co-expression or homology. The task is to predict the presence of protein functions in a multi-label binary classification setup, where there are 112 kinds of protein functions denote as labels to predict in total. Here the protein functions refer to the specific biological activities or roles that a protein performs within a cell or organism. These functions are typically described using Gene Ontology (GO) database Huntley et al. (2015) or other biological annotation systems and can fall into different categories.
- PCG Zhao et al. (2023) is Protein-Phenotype graph dataset, which focused on predicting phenotypes associated with proteins. Phenotypes refer to observable traits or characteristics of diseases, and identifying these associations can be valuable for clinical diagnostics or discovering potential drug targets. The dataset is constructed using protein-phenotype associations from the DisGeNET database Piñero et al. (2020), where each protein is linked to one or more phenotypes. The phenotypes are grouped into disease categories based on the MESH ontology Bhattacharya et al. (2011), and labels with fewer than 100 associated proteins are removed. The PCG includes 3,233 proteins as nodes and

37,351 protein-protein interactions as edges. The task is to predict multiple phenotype labels for each protein based on its interactions and features.

- HumanGo Chou & Shen (2007); Liberzon et al. (2015) contains 3,106 proteins, each potentially associated with one or more of 14 subcellular locations as multi-label. The proteins are represented as nodes in a graph, with features generated from their sequences using pre-trained model Yang et al. (2020). Protein-protein interactions form the edges of the graph, with each edge representing the confidence of different interaction types. Different location associations come from the GO database Huntley et al. (2015), which assigns standardized terms to proteins based on their roles in biological processes (e.g., cell division, metabolism), molecular functions (e.g., enzyme activity, receptor binding), and cellular components (e.g., nucleus, membrane).
- EukaryoteGo Chou & Shen (2007); Liberzon et al. (2015) follows a similar structure but focuses on eukaryote proteins. It includes 7,766 proteins and their interactions, with proteins being assigned to one or more of 22 subcellular locations. Like HumanGo, it uses protein sequences for node features and protein-protein interactions for graph structure.

We follow the predefined data splits from Zeng et al. (2019); Zhao & Bilen (2023); Hu et al. (2020); Chou & Shen (2007). 1 presents an overview of the datasets’ characteristics.

Table 1: Dataset Statistics

Dataset	#Nodes	#Edges	#Avg.Edges	#Features	#Labels	Train/Val/Test
<b>PPI</b>	14,755	225,270	15.27	50	121	0.66/0.12/0.22
<b>PPI-large</b>	56,944	818,716	14.38	50	121	0.79/0.11/0.10
<b>Yelp</b>	716,847	6,977,410	9.73	300	100	0.75/0.10/0.15
<b>DBLP</b>	28,702	68,335	2.38	300	4	0.60/0.20/0.20
<b>OGBN-Proteins</b>	132,000	39,000,000	295.45	8	112	0.66/0.16/0.18
<b>PCG</b>	3,233	37,351	11.55	32	15	0.60/0.20/0.20
<b>HumanGo</b>	3,106	18,496	5.96	32	14	0.60/0.00/0.40
<b>EukaryoteGo</b>	7,766	13,818	1.78	32	22	0.60/0.00/0.40

**Metrics.** To evaluate the performance of adapted graph condensation methods, we utilize two widely recognized metrics in multi-label classification: F1-micro and F1-macro.

- F1-micro score aggregates the contributions of all classes to compute the average F1 score. It does this by first calculating the total true positives, false positives, and false negatives across all labels, and then using these aggregated values to compute a global precision and recall. The F1-micro score is particularly useful when dealing with imbalanced datasets, as it gives equal weight to each instance rather than each class. It is defined as:

$$\text{F1-micro} = \frac{2 \times \text{Precision} \times \text{Recall}}{\text{Precision} + \text{Recall}} \tag{14}$$

where:

$$\text{Precision} = \frac{\text{TP}}{\text{TP} + \text{FP}}$$

$$\text{Recall} = \frac{\text{TP}}{\text{TP} + \text{FN}}$$

- F1-macro score computes the F1 score for each class independently and then averages these scores. This metric treats all classes equally, regardless of their frequency in the dataset. It is particularly useful for understanding the model’s performance across all classes, especially in scenarios where some classes may be underrepresented. The F1-macro score is defined as:



Datasets	C-rate	Random		Herding		K-Center		Probability	Whole Dataset
		Subgraph	Nodes	Subgraph	Nodes	Subgraph	Nodes		
PPI	1.00%	47.05	<b>40.49</b>	40.93	39.47	<b>47.77</b>	36.60	40.04	51.26
Yelp	0.02%	34.21	30.35	32.77	30.96	<b>35.60</b>	<b>31.46</b>	20.95	37.97
DBLP	0.80%	<b>63.56</b>	<b>56.03</b>	41.54	41.02	60.36	55.62	41.35	87.55
OGBN-Proteins	0.1%	14.12	15.44	11.62	15.36	<b>29.95</b>	<b>24.81</b>	15.53	18.86
PCG	4%	13.94	19.01	<b>27.76</b>	16.35	25.13	<b>22.18</b>	21.69	42.26

Table 2: F1-Micro Score (%) of Coreset Method with Different Initialization Strategies

Datasets	C-rate	Random		Herding		K-Center		Probability		Whole Dataset
		Without $A'$	With $A'$	Without $A'$	With $A'$	Without $A'$	With $A'$	Without $A'$	With $A'$	
PPI	1.00%	<b>48.55</b>	<b>50.17</b>	46.71	47.80	35.99	48.38	44.62	43.31	51.26
Yelp	0.02%	30.16	29.53	30.48	32.23	<b>34.50</b>	<b>34.90</b>	21.33	22.10	37.97
DBLP	1%	52.10	57.48	45.95	47.12	<b>52.56</b>	<b>60.77</b>	48.24	48.56	87.55
OGBN-Proteins	0.10%	22.03	28.69	20.54	25.19	<b>28.09</b>	<b>29.04</b>	22.10	27.01	30.59
PCG	4%	20.50	23.79	<b>22.14</b>	25.38	19.88	22.36	22.07	<b>27.21</b>	42.26

Table 3: F1-Micro Score (%) of GCond Method with Random/Herding/K-Center/Probability Distribution Initialization with/without Learning from Structure for SoftMarginLoss.

$$F1\text{-macro} = \frac{1}{C} \sum_{i=1}^C F1_i \quad (15)$$

where  $C$  is the number of classes and  $F1_i$  is the F1 score for the  $i^{th}$  class, calculated as:

$$F1_i = \frac{2 \times \text{Precision}_i \times \text{Recall}_i}{\text{Precision}_i + \text{Recall}_i} \quad (16)$$

After introduce the single-label graph condensation methods, we will focus on adjusting key components to fit the multi-label task while preserving the core matching mechanisms. This ensures that our framework can be extended to other existing graph condensation techniques, allowing for flexible and efficient adaptation across different methods. This benchmark presents a thorough evaluation of the various settings and methods used for graph condensation in the multi-label scenario. We structure the benchmark results into three key parts: (1) identifying the best initialization and loss function settings, (2) comparing the full results of all graph condensation methods across multiple datasets, and (3) analyzing the results through multi-label class distribution and label correlation.

## 6 Adapt Existing Graph Condensation Methods for Multi-label Datasets

After the introduction of different graph condensation methods based on the matching strategies in Section 4 including GCond, SGDD and GCDM, we apply the above methods in multi-label graph datasets in this section. However, these methods could not directly be applied to condense multi-label graphs majorly due to two reasons: (1) The synthetic graph initialization is designed for single-class augmentation with pre-defined condensed labels. (2) The condensation methods depend on GNNs to match the original graph  $\mathcal{G}$  and synthetic graph  $\mathcal{S}$ , the classification objectives are designed for single-label node classification. Therefore, in this section, we would like to adapt the existing graph condensation methods by investigating different

Datasets	C-rate	Random		Herding		K-Center		Probability		Whole Dataset
		Without $A'$	With $A'$	Without $A'$	With $A'$	Without $A'$	With $A'$	Without $A'$	With $A'$	
PPI	1.00%	<b>49.95</b>	<b>51.35</b>	47.47	48.23	36.79	49.27	45.65	43.91	51.26
Yelp	0.02%	29.24	30.76	31.76	32.41	<b>32.36</b>	<b>33.94</b>	22.96	25.62	37.97
DBLP	1%	53.41	59.40	46.87	48.50	<b>54.21</b>	<b>70.74</b>	49.73	51.33	87.55
OGBN-Proteins	0.10%	24.65	28.88	21.45	26.21	<b>28.15</b>	<b>29.40</b>	21.73	27.11	30.59
PCG	4%	22.26	25.45	<b>24.66</b>	26.76	20.17	25.58	23.47	<b>28.28</b>	42.26

Table 4: F1-Micro Score (%) of GCond Method with Random/Herding/K-Center/Probability Initialization with/without Learning from Structure for BCELoss.

adaptation strategies to address these two issues. In particular, we first describe the existing issues and the corresponding resolvents in Section 6.1. Then, we conduct experiments to investigate which strategies work best for the multi-label graph condensation tasks in Section 6.2.

## 6.1 Multi-label Adaptation

During condensation stage, among all the condensation methods, class-wise batch sampling is widely used for synthetic graph optimization. For instance, in GCond, they initialize the synthetic graph labels  $Y'$  by predefine the labels for each class with condensation rate  $r$ . While optimization, to further reduce the memory usage and simplify the process, they calculate the gradient matching loss for nodes from different classes separately. As matching the gradients from a single class is easier than from all the classes, most of condensation researches follow this class-wise sampling method. However, in contrast to a single-labeled graph, a multi-labeled graph has multiple class labels assigned to each node, so the class-wise initialization and optimization process need to be revised to the multi-label scenario. Furthermore, when adapting single-label graph condensation techniques to multi-label node classification, the choice of the loss function is crucial to ensuring that the model effectively learns the complex relationships inherent in multi-label tasks. In single-label graph condensation, methods typically optimize for cross-entropy loss, which is suitable for tasks where each node belongs to a single class. However, in multi-label classification, nodes can belong to multiple classes simultaneously.

Therefore, to better determine the best setting for multi-label graph condensation we investigate different initialization and optimization methods to evaluate their impact on preserving multi-label relationships and classification accuracy.

Our objective is to assess how these initialization methods and loss functions influence the performance of the condensed graphs in multi-label classification tasks. To sum up, we focus on two key areas of adaptation: **initialization** and **optimization** of the synthetic graph. These modifications allow us to capture and preserve the essential multi-label features of the original graph.

**Issue 1: Initialization of Synthetic Multi-Label Graph.** In single-label settings, the condensed label  $Y'_{single}$  is predefined using ground-truth class distribution and retrieves  $X'$  randomly from each class.

As most of the graph condensation methods adapt Eq.6 to learn synthetic graph structure  $A'$  from node features  $X'$ , one straightforward method for multi-label adaptation is sampling the nodes from original datasets. Inspired by the heuristic sampling algorithms of baseline Coreset methods used in GCond, the sampled subgraph by different strategies can be used for the synthetic multi-label initialization to get a better performance.

As some of the coreset methods gain comparable performance as baseline Welling (2009); Farahani & Hekmatfar (2009); Sener & Savarese (2017), we apply those heuristic algorithms to extract  $N'$  nodes from the full set of nodes to obtain subgraphs  $S'$  with corresponding condensation rates as the initialization methods.

- Random selection is sampling the nodes randomly, so the probability of selecting node  $i$  is  $P(i) = \frac{1}{N}$ .
- Herding Welling (2009) method is more structured compared with random selection strategy. It is based on iterative minimization of the distance between the mean of the selected nodes' feature vectors and the mean of the entire graph feature vectors. Let  $\mu_G$  present the mean feature vector of the original graph:

$$\mu_G = \frac{1}{N} \sum_{i=0}^{N-1} x_i \quad \text{and} \quad \mu_S = \frac{1}{N'} \sum_{j=0}^{N'-1} x'_j \quad (17)$$

- K-Center Farahani & Hekmatfar (2009); Sener & Savarese (2017) method aims to maximize the coverage of the original graph feature space by minimizing the maximum distance between unselected nodes and their closest selected node. Let  $\mathcal{S} = \{s_1, s_2, \dots, s_{N'}\}$  be the selected node set. The goal is to select nodes such that for every unselected node  $i$ , the distance to the nearest selected node  $s_j \in \mathcal{S}$  is minimized:

$$\min_{s_1, \dots, s_{N'}} \max_{i \in \{1, \dots, N\}} \min_{j \in \{1, \dots, N'\}} \|x_i - x_{s_j}\|_2 \quad (18)$$

The selection process would start from an arbitrary node as the first center  $s_1$  and then iteratively select the next node  $s_t$  which is farthest away from the selected nodes. The process continues until  $N'$  nodes are selected.

- In the multi-label scenario, each node has multiple labels, and it is also important to ensure that the selected subgraph maintains the label distribution of the original graph. Here, we introduce probabilistic synthetic multi-label method, for each class  $k$ , define the label distribution as the fraction of nodes in the graph that belongs to class  $k$ :

$$p_k = \frac{1}{N} \sum_{i=1}^N Y_{i,k} \quad (19)$$

The goal is to ensure that the synthetic graph  $\mathcal{S}$  maintains a similar label distribution. So for each synthetic label  $y'_j$  in  $Y' \in 0, 1^{N' \times K}$ , the label of class  $k$  has a  $p_k$  probability to be 1. Then we choose cosine similarity matching for the node features based on the real labels from  $\mathcal{G}$  and probability synthetic labels.

Above all, in multi-label settings, we adapt subgraph initialization and probabilistic synthetic multi-label methods for multi-label graph condensation. Besides, in graph condensation, the structure  $A'$  of synthetic graph is optimized from nodes features  $X'$ . Based on the researches Ding et al. (2022); Zhu et al. (2021); Jin et al. (2022b), this "Graphless" learning process can be highly useful for downstream data analysis, which also shows competitive performance. Therefore, by comparing different initialization methods with or without learning the graph structure, we get the best settings for the adaptation.

## Issue 2: Optimization about Multi-Label Classification Loss.

In single-label settings, while the condensed graph is matched in various ways, the fixed label distribution can be used directly for synthetic graph initialization. With predefined synthetic label  $Y'_{single} \in \{0, \dots, C-1\}^{N'}$ , the synthetic node feature is randomly retrieved from the particular class. As calculate the matching loss for nodes from different classes separately, is easier than that from all classes. In other words, this single-label class-wise sample method will directly sample each class to optimize. Specifically, for a given class  $c$ , it will sample a batch of nodes of class  $c$  from original graph  $\mathcal{G}$  with a portion of neighbors, denotes as  $(A_c, X_c, Y_c) \sim \mathcal{G}$ . For synthetic graph  $\mathcal{S}$ , only sample the specific nodes of class  $c$  without the neighbors. By doing so, the synthetic graph will use all the other nodes for aggregation stages during condensation, similarly, this process can be wrote as  $(A'_c, X'_c, Y'_c) \sim \mathcal{S}$ . Further in terms of details, for each class  $c$ , there is a subset of nodes  $N_c$  that belong to this class. The loss is computed class-wise, for example, the cross-entropy loss for single node  $j$  with ground truth label  $y_j$  and predicted logit  $z_{j,c}$  for class  $c$  is:

$$\ell_{CE}(z_j, y_j) = -\log\left(\frac{e^{z_{j,y_j}}}{\sum_{c=0}^{C-1} e^{z_{j,c}}}\right) \quad (20)$$

The single-label final loss would be formulated as:

$$\mathcal{L}_{single-label} = \sum_{c=0}^{C-1} \sum_{j \in N_c} \ell_{CE}(z_j, y_j) \quad (21)$$

However, in multi-label classification  $Y' \in \{y'_1, \dots, y'_N\} \in \{0, 1\}^{N' \times K}$ , each node can associate with multiple classes simultaneously. Typically, the multi-label classification task is modeled as  $K$  independent binary classification tasks, for each task  $k$ , the model predicts a logit  $z_{j,k}$  and ground-truth label  $y_{j,k}$  indicates whether node  $j$  belongs to class  $k$ . In multi-label classification, SoftMarginLoss Cao et al. (2019) incorporates margin-based optimization, which is beneficial when dealing with imbalanced datasets and overlapping classes. In multi-label settings, certain labels may frequently co-occur or exhibit correlations. SoftMarginLoss introduces a margin between positive and negative label predictions, encouraging the model to differentiate between these labels more confidently.

$$\mathcal{L}_{Softmargin}(z_{j,k}, y_{j,k}) = \log(1 + e^{-z_{j,k} \cdot y_{j,k}}) \quad (22)$$

This formulation is particularly useful in ensuring that the model not only predicts correct labels but does so with confidence, reducing the chances of ambiguous predictions near the decision boundary. On the other hand, Binary Cross-Entropy Loss Durand et al. (2019) is a widely-used objective function for multi-label classification, as it independently evaluates each label for each node in the graph. Then the task-wise loss for each binary classification task is computed using Binary Cross-Entropy (BCE) Durand et al. (2019) loss:

$$\mathcal{L}_{\text{BCE}}(z_{j,k}, y_{j,k}) = -(y_{j,k} \log(\sigma(z_{j,k})) + (1 - y_{j,k}) \log(1 - \sigma(z_{j,k}))), \quad (23)$$

where  $\sigma(z_{j,k}) = \frac{1}{1+e^{-z_{j,k}}}$  is the sigmoid function.

## 6.2 Experiments and Results Analysis

In this section, after the investigation of different initialization and optimization strategies. We combine them together to find out the best settings for multi-label graph condensation adaptation. Additional results in terms of other metrics are presented in Appendix A.

In this section, we conduct experiments on GCond to investigate the effectiveness of different initialization and optimization strategies on the representative datasets and corresponding condensation rates. We first introduce the experiment settings with specific methods and datasets. In graph condensation, the condensation ratio (often denoted as C-rate) is a measure of how much the original graph has been reduced in size for training purposes. This ratio represents the percentage or fraction of nodes retained from the full dataset in the condensed graph. For example, if the C-rate is set to 1%, it means that the scale of synthetic graph  $\mathcal{S}$  is only 1% of original graph  $\mathcal{G}$ . Then we statistically analyzed the experimental results and presented the comparison of different settings for multi-label graph condensation.

**Settings.** For dataset selection, we pick the most representative datasets to simplify the choosing stage, for instance, PPI-large is the larger version of PPI dataset, so we only test the settings in PPI. With the representative datasets, we choose the C-rate based on the number of nodes in synthetic graph to compare the performance. Take the PPI dataset as the example, C-rate equals 1.00% means the synthetic graph has 147 nodes compared with original 14755 nodes. For all the synthetic graphs, the nodes number is around 150.

Specifically, we report the performance of various initialization strategies include subgraph sampling( Random, Herding, K-Center) Welling (2009); Farahani & Hekmatfar (2009); Sener & Savarese (2017), and probabilistic label sampling for synthetic  $Y'$ . After the initialization, the synthetic graph  $\mathcal{S}$  will be optimized by gradient matching strategy in GCond. Then we compare different optimization loss functions, including SoftMarginLoss Cao et al. (2019) and BCE loss Durand et al. (2019), across diverse datasets with pre-choosen condensation rates. Through these experiments, we aim to identify the optimal combination of initialization and loss function that achieves the best trade-off between graph size reduction and model performance in multi-label tasks.

**Results and Analysis.** Finally, by comparing different settings of multi-label scenario on GCond framework, we present the corresponding results of above initialization and optimization with or without structure learning. Specifically, Table 2 shows the F1-micro scores for four initialization strategies (Random, Herding, K-Center, and Probability) applied to both subgraph and node-only settings. This comparison across datasets allows us to identify which strategies best capture label distributions in multi-label tasks. Then Table 3, 4 compare performance under SoftMarginLoss and BCELoss optimizations, respectively. Besides, for each initialization method we investigate the performance of synthetic graph with or without structure information. These results help to pinpoint effective combinations of initialization and loss functions.

After analysis of the overall performance with key observations, we report the best setting for multi-label adaptation to better generalization in other methods. By observing the experimental results, we draw three corresponding observation conclusions:

**Observation 1: K-Center sampling achieves optimal initialization.**

In the GCond framework, K-Center sampling consistently provides the highest F1-micro scores for dense, large-scale datasets such as PPI, Yelp, and OGBN-Proteins in Tables 2, 3, 4.

---

In contrast, simpler strategies like Random and Herding yield better results in datasets with lower density, such as DBLP and PCG.

Following initialization, we tested SoftMarginLoss and BCELoss for optimization. Table 3 and Table 4 are the comparison of different initialization methods optimized by SoftMarginLoss and BCELoss, respectively. Whole dataset indicates the performance of GNN trained by original graph  $\mathcal{G}$ . (a) and (b) are the comparison of learning condensed graph with or without structure  $A'$ . We present the combined bar and line chart to show a more intuitive comparison of the differences between various combinations of initialization and optimization methods. Interestingly, we find the best performance distribution is consistency even using different loss functions. K-Center initialization with or without graph structure optimization gains the best performance using BCELoss. In particular, datasets like PPI and DBLP exhibit notable performance gaps that highlight the advantage of structure learning (per Eq.6) in enhancing multi-label generalization.

**Observation 2: Preserving graph structure could improve performance of condensed large datasets.** We examined the effects of learning graph structure versus using nodes alone for label initialization. Results show substantial performance improvements when the graph structure is preserved, especially in large-scale datasets. While all the experiments are conducted with the comparison of learning synthetic graph with or without structure information, we find out that with the additional  $A'$  learning, the condensed graph would perform better in the large-scale datasets.

Before condensation the structure information already shows its effectiveness. For example, in the comparison of initialization methods present in Table 2 PPI with a sampling of the C rate of 1.00% and the K-Center, retaining the structure achieves an F1 micro score of 47.77%, compared to 36.60% with nodes alone. During condensation process, optimization with the structure information learning, same pattern is observed across various methods (see Table 3, 4 for a comparison with or without  $A'$  learning process), demonstrating the critical role of structural information.

**Observation 3: BCELoss provides better overall results** When comparing loss functions, BCELoss generally yields higher F1-micro scores, especially when combined with structure learning. For example, In Table 4, the DBLP dataset with K-Center sampling and structure learning, BCELoss achieves an F1-micro score of 70.74%, substantially outperforming the SoftMarginLoss score of 60.77%. This trend is consistent across multiple datasets, highlighting BCELoss as the optimal choice for multi-label adaptation in GCond.

Across all initialization settings, the subgraph sampled by the K-Center strategy receives the best performance in the PPI, Yelp and OGBN-Proteins rating by F1-micro score. However, Random and Herding work quite well among the less dense multi-label datasets like DBLP and PCG. After removing the graph structure, by comparing only the set of nodes of the sampled graphs for label initialization and probability synthetic labels in Table 2, we find that some of the graph structure could have a factor to impact performance like in PPI with 1.00% using K-Center, the result of the subgraph could achieve 47.77% with structure while 36.60% only with nodes. Similarly, K-Center works best among Yelp, OGBN-Proteins, and PCG with node set. Probability synthetic labels capture less of the distribution of the multi-labels in original dataset and only get comparable performance in PPI. After deploying the initialization methods, we also compare these various settings combined with the loss functions discussed. Following the optimization of the condensation process with or without  $A'$ , we report the results of GCond with SoftMarginLoss and BCELoss optimization strategies in Table 3 and Table 4, respectively. Finally, we report the general initialization methods comparison visually and F1-macro score in appendix A. Interestingly, we find the best performance distribution is consistency even using different loss functions. K-Center initialization with or without graph structure optimization gains the best performance using BCELoss. Noticeably, based on structure learning in Eq.6 the performance gap is quite obvious in PPI and DBLP datasets.

*Consistent with Observations 1 and 2, initializing with K-Center sampling and incorporating structure learning  $A'$  could increase the performance of synthetic multi-label graph. As shown in Observation 3, across a variety of datasets, BCELoss performs better than SoftMarginLoss. Particularly when paired with K-Center and structural learning, BCELoss improves the F1-micro score, suggesting it can offer greater label retention and general adaptability. Therefore, we adopt the K-Center and BCELoss as the initialization and optimization methods with structure information for multi-label scenario.*

## 7 Benchmarking

Table 5: Graph Condensation Methods Performance Comparison with F1-micro and F1-macro. Performance metrics of the model, with the F1-score represented as a decimal value. "-" means the out-of-memory (OOM) errors.

Dataset	C-rate	Coreset (Random)		Coreset (Herding)		Coreset (K-Center)		SGDD		GCDM		GCond		Whole Dataset	
		F1-micro	F1-macro	F1-micro	F1-macro	F1-micro	F1-macro	F1-micro	F1-macro	F1-micro	F1-macro	F1-micro	F1-macro	F1-micro	F1-macro
PPI	<b>0.50%</b>	41.92	14.69	41.16	12.76	45.65	15.54	44.99	22.58	48.28	23.37	<b>49.63</b>	<b>23.16</b>	51.26	30.06
	<b>1.00%</b>	39.07	12.58	41.23	11.66	47.43	17.36	47.02	18.26	47.07	21.76	<b>51.35</b>	<b>23.86</b>		
	<b>2.00%</b>	41.12	14.12	39.21	10.23	<b>52.34</b>	<b>26.62</b>	46.73	21.24	47.91	21.93	51.21	24.32		
PPI-large	<b>0.10%</b>	44.43	14.49	43.17	13.74	41.12	18.11	49.32	18.33	47.13	37.59	<b>51.05</b>	<b>27.51</b>	51.61	28.23
	<b>0.20%</b>	45.15	15.80	43.39	15.91	40.88	13.00	44.82	15.78	46.26	22.24	<b>51.99</b>	<b>29.95</b>		
	<b>0.40%</b>	44.01	15.43	43.61	13.74	41.04	12.89	49.89	29.08	44.08	19.48	<b>52.23</b>	<b>28.59</b>		
Yelp	<b>0.01%</b>	33.73	5.55	33.63	7.07	<b>34.20</b>	<b>13.30</b>	-	-	28.00	2.78	28.40	7.51	37.97	15.18
	<b>0.02%</b>	33.64	5.09	32.94	5.64	<b>35.64</b>	<b>12.30</b>	-	-	27.84	3.76	33.94	6.22		
	<b>0.04%</b>	34.01	5.41	32.87	4.67	<b>36.51</b>	<b>12.51</b>	-	-	26.42	2.87	32.77	5.85		
	<b>0.05%</b>	33.74	5.86	32.83	5.17	<b>36.63</b>	<b>11.30</b>	-	-	24.10	2.42	34.11	6.86		
	<b>0.10%</b>	33.56	5.19	32.83	5.51	<b>36.65</b>	<b>9.79</b>	-	-	24.82	2.95	33.70	8.17		
	<b>0.20%</b>	33.75	5.50	33.20	4.71	<b>37.61</b>	<b>11.48</b>	-	-	28.43	3.32	32.41	12.18		
DBLP	<b>0.20%</b>	49.28	34.81	41.02	15.41	52.70	49.75	43.17	25.06	44.41	34.84	<b>63.36</b>	<b>56.27</b>	87.55	86.39
	<b>0.40%</b>	52.94	44.71	42.59	31.05	55.27	50.89	45.37	43.42	45.88	26.54	<b>68.11</b>	<b>57.35</b>		
	<b>0.80%</b>	62.08	56.00	41.11	15.63	59.77	56.90	43.48	25.42	46.66	46.20	<b>70.74</b>	<b>68.44</b>		
	<b>1.60%</b>	68.39	63.75	42.24	25.78	63.87	62.34	42.73	34.22	45.99	26.47	<b>70.49</b>	<b>68.92</b>		
OGBN-Proteins	<b>0.05%</b>	14.40	1.70	11.29	4.25	<b>28.74</b>	<b>7.83</b>	-	-	21.82	7.95	26.38	9.98	10.14	9.16
	<b>0.10%</b>	15.63	2.12	15.28	5.21	<b>31.04</b>	<b>10.13</b>	-	-	22.18	3.07	29.40	7.47		
	<b>0.20%</b>	16.90	2.06	8.55	1.64	<b>26.36</b>	<b>4.82</b>	-	-	21.38	8.78	<b>29.26</b>	<b>7.71</b>		
PCG	<b>2.00%</b>	15.72	5.57	18.98	3.03	27.44	9.09	27.93	15.32	<b>29.48</b>	<b>13.22</b>	18.84	14.21	42.26	31.49
	<b>4.00%</b>	15.83	5.20	23.03	13.84	25.13	5.73	28.40	9.00	<b>32.16</b>	<b>8.31</b>	25.58	13.32		
	<b>8.00%</b>	16.67	3.02	22.48	9.36	18.21	4.59	<b>33.50</b>	<b>8.58</b>	31.88	12.51	26.37	13.90		
HumanGo	<b>2.00%</b>	28.88	4.57	19.92	4.39	25.38	6.15	35.58	10.06	<b>36.71</b>	<b>6.53</b>	30.68	11.24	51.67	25.57
	<b>4.00%</b>	27.95	7.98	31.70	6.66	31.94	7.24	35.39	9.19	<b>35.79</b>	<b>7.31</b>	34.91	10.74		
	<b>8.00%</b>	<b>37.57</b>	<b>9.58</b>	32.44	5.50	36.50	7.67	35.25	9.74	36.54	7.35	37.18	12.05		
EukaryoteGo	<b>1.00%</b>	31.45	5.57	21.60	4.24	17.79	2.66	29.40	3.25	<b>36.83</b>	<b>4.09</b>	35.24	5.57	45.86	12.27
	<b>2.00%</b>	30.72	5.03	26.74	5.16	20.99	3.03	28.69	3.28	<b>36.98</b>	<b>4.09</b>	36.38	7.00		
	<b>3.00%</b>	30.79	4.18	25.99	3.43	22.08	4.31	36.57	4.75	36.97	4.84	<b>38.90</b>	<b>6.04</b>		

In this section, followed the best setting discussed in Section 6, we adapt all the discussed condensation methods into multi-label scenario based on the former settings. The results in Table 5 illustrate the efficacy of different Coreset selection strategies (Random, Herding, K-Center) and graph condensation methods (SGDD, GCDM, GCond) compared to the full dataset. The comparison is performed at different condensation rates (C-rate), providing insights into the impact of these methods on classification performance in multi-label tasks. Specifically, SGDD and GCond both choosing gradient matching for the GNNs trained on original graph  $\mathcal{G}$  and synthetic graph  $\mathcal{S}$  directly. GCDM uses the embedding matching based on the nodes set belongs to the same class in multi-label.

We have several noteworthy observations concerning the methods, the datasets, the evaluation settings, and the overall results. We highlight the main observations below. Here, the performance metrics of the model, with the F1-score represented as a decimal value.

**Observation 1: GCond achieves the best results across datasets.** GCond consistently outperforms other methods on most datasets, particularly excelling in large-scale datasets with substantial label complexity. On the PPI dataset, GCond achieves F1-micro and F1-macro scores of 51.35% and 23.86%, respectively, at a 1.00% condensation rate. This robustness extends to PPI-large, where it achieves scores of 52.23% (F1-micro) and 28.59% (F1-macro) at a 0.40% condensation rate. Similarly, on DBLP, GCond demonstrates its superiority with F1-micro and F1-macro scores of 70.74% and 68.44%, respectively, at 0.80% condensation, showcasing its ability to preserve label correlations and structural integrity during condensation. However, GCond’s advantage diminishes in the Yelp dataset at high condensation levels, likely due to the dataset’s unique label structure, which poses challenges for methods relying on label coherence preservation.

**Observation 2: K-Center demonstrates stability in extreme condensation setting.** The K-Center method shows consistent performance, particularly on large-scale and dense-label datasets, highlighting its strength in preserving diversity at low condensation rates. On the Yelp dataset, K-Center outperforms traditional Coreset methods, achieving the highest F1-micro score (37.61%) at a 0.20% condensation rate. This suggests that its selection strategy effectively retains essential structural and label information, even under high condensation, making it advantageous for large-scale settings where extreme data reduction risks losing critical information.

**Observation 3: SGDD’s performance is constrained by scalability issues on larger datasets.** SGDD faces out-of-memory (OOM) errors on large datasets like Yelp and OGBN-Proteins, revealing its scalability limitations. However, on smaller datasets, SGDD performs competitively, benefiting from its

---

structure-broadcasting graphon technique, which efficiently captures structural patterns. For example, on datasets such as PCG, HumanGo, and EukaryoteGo, SGDD achieves strong F1-micro and F1-macro scores, demonstrating its effectiveness on smaller scales. Nevertheless, its applicability to larger datasets requires further optimization.

In conclusion, the efficacy of each condensation method varies depending on the characteristics of the dataset. GCond’s superior performance on complex, high-dimensional datasets such as DBLP and PPI demonstrates its strong alignment with datasets that require maintaining label consistency and intricate relationships. In contrast, simpler methods like Random and Herding exhibit relatively stable performance but are outperformed by GCond and K-Center on datasets where preserving structure and label diversity is critical. These findings underscore the importance of selecting methods based on dataset scale, complexity, and label interaction patterns.

## 8 Conclusion

In this benchmark, we presented a comprehensive framework for multi-label graph condensation, adapting traditional single-label methods to address the complexities inherent in multi-label classification tasks. The results show that the GCond method not only excels in maintaining the structural integrity of the original graph, but also enhances the label correlations, leading to more accurate multi-label predictions.

## References

- Uchenna Akujuobi, Han Yufei, Qiannan Zhang, and Xiangliang Zhang. Collaborative graph walk for semi-supervised multi-label node classification. In *2019 IEEE International Conference on Data Mining (ICDM)*, pp. 1–10. IEEE, 2019.
- Peter W Battaglia, Jessica B Hamrick, Victor Bapst, Alvaro Sanchez-Gonzalez, Vinicius Zambaldi, Mateusz Malinowski, Andrea Tacchetti, David Raposo, Adam Santoro, Ryan Faulkner, et al. Relational inductive biases, deep learning, and graph networks. *arXiv preprint arXiv:1806.01261*, 2018.
- Sanmitra Bhattacharya, Viet Ha-Thuc, and Padmini Srinivasan. Mesh: a window into full text for document summarization. *Bioinformatics*, 27(13):i120–i128, 2011.
- Aleksandar Bojchevski, Johannes Gasteiger, Bryan Perozzi, Amol Kapoor, Martin Blais, Benedek Rózemberczki, Michal Lukasik, and Stephan Günnemann. Scaling graph neural networks with approximate pagerank. In *Proceedings of the 26th ACM SIGKDD International Conference on Knowledge Discovery & Data Mining*, pp. 2464–2473, 2020.
- Kaidi Cao, Colin Wei, Adrien Gaidon, Nikos Arechiga, and Tengyu Ma. Learning imbalanced datasets with label-distribution-aware margin loss. *Advances in neural information processing systems*, 32, 2019.
- Zhao-Min Chen, Xiu-Shen Wei, Peng Wang, and Yanwen Guo. Multi-label image recognition with graph convolutional networks. In *Proceedings of the IEEE/CVF conference on computer vision and pattern recognition*, pp. 5177–5186, 2019.
- Avery Ching, Sergey Edunov, Maja Kabiljo, Dionysios Logothetis, and Sambavi Muthukrishnan. One trillion edges: Graph processing at facebook-scale. *Proceedings of the VLDB Endowment*, 8(12):1804–1815, 2015.
- Kuo-Chen Chou and Hong-Bin Shen. Euk-mploc: a fusion classifier for large-scale eukaryotic protein subcellular location prediction by incorporating multiple sites. *Journal of Proteome Research*, 6(5): 1728–1734, 2007.
- Kenneth Ward Church. Word2vec. *Natural Language Engineering*, 23(1):155–162, 2017.
- Kinkar Ch Das, Seyed Ahmad Mojallal, and Vilmar Trevisan. Distribution of laplacian eigenvalues of graphs. *Linear Algebra and its Applications*, 508:48–61, 2016.

- 
- Kaize Ding, Zhe Xu, Hanghang Tong, and Huan Liu. Data augmentation for deep graph learning: A survey. *ACM SIGKDD Explorations Newsletter*, 24(2):61–77, 2022.
- Yingtong Dou, Zhiwei Liu, Li Sun, Yutong Deng, Hao Peng, and Philip S Yu. Enhancing graph neural network-based fraud detectors against camouflaged fraudsters. In *Proceedings of the 29th ACM international conference on information & knowledge management*, pp. 315–324, 2020.
- Thibaut Durand, Nazanin Mehrasa, and Greg Mori. Learning a deep convnet for multi-label classification with partial labels. In *Proceedings of the IEEE/CVF conference on computer vision and pattern recognition*, pp. 647–657, 2019.
- David K Duvenaud, Dougal Maclaurin, Jorge Iparraguirre, Rafael Bombarell, Timothy Hirzel, Alán Aspuru-Guzik, and Ryan P Adams. Convolutional networks on graphs for learning molecular fingerprints. *Advances in neural information processing systems*, 28, 2015.
- Reza Zanjirani Farahani and Masoud Hekmatfar. *Facility location: concepts, models, algorithms and case studies*. Springer Science & Business Media, 2009.
- Hongyang Gao, Zhengyang Wang, and Shuiwang Ji. Large-scale learnable graph convolutional networks. In *Proceedings of the 24th ACM SIGKDD international conference on knowledge discovery & data mining*, pp. 1416–1424, 2018.
- Shuang Gao and Peter E Caines. Graphon control of large-scale networks of linear systems. *IEEE Transactions on Automatic Control*, 65(10):4090–4105, 2019.
- Xinyi Gao, Junliang Yu, Wei Jiang, Tong Chen, Wentao Zhang, and Hongzhi Yin. Graph condensation: A survey. *arXiv preprint arXiv:2401.11720*, 2024.
- Yang Gao, Hong Yang, Peng Zhang, Chuan Zhou, and Yue Hu. Graph neural architecture search. In *International joint conference on artificial intelligence*. International Joint Conference on Artificial Intelligence, 2021.
- Ivan Gutman and Bo Zhou. Laplacian energy of a graph. *Linear Algebra and its applications*, 414(1):29–37, 2006.
- Will Hamilton, Zhitao Ying, and Jure Leskovec. Inductive representation learning on large graphs. *Advances in neural information processing systems*, 30, 2017.
- William L. Hamilton, Rex Ying, and Jure Leskovec. Inductive representation learning on large graphs, 2018. URL <https://arxiv.org/abs/1706.02216>.
- Mohammad Al Hasan and Mohammed J Zaki. A survey of link prediction in social networks. *Social network data analytics*, pp. 243–275, 2011.
- Mohammad Hashemi, Shengbo Gong, Juntong Ni, Wenqi Fan, B. Aditya Prakash, and Wei Jin. A comprehensive survey on graph reduction: Sparsification, coarsening, and condensation. *ArXiv*, abs/2402.03358, 2024. URL <https://api.semanticscholar.org/CorpusID:267341687>.
- Weihua Hu, Matthias Fey, Marinka Zitnik, Yuxiao Dong, Hongyu Ren, Bowen Liu, Michele Catasta, and Jure Leskovec. Open graph benchmark: Datasets for machine learning on graphs. *arXiv preprint arXiv:2005.00687*, 2020.
- Sheng-Jun Huang and Zhi-Hua Zhou. Multi-label learning by exploiting label correlations locally. In *Proceedings of the AAAI Conference on Artificial Intelligence*, volume 26, pp. 949–955, 2012.
- Rachael P Huntley, Tony Sawford, Prudence Mutowo-Meullenet, Aleksandra Shypitsyna, Carlos Bonilla, Maria J Martin, and Claire O’Donovan. The goa database: gene ontology annotation updates for 2015. *Nucleic acids research*, 43(D1):D1057–D1063, 2015.



- 
- Dejun Jiang, Zhenxing Wu, Chang-Yu Hsieh, Guangyong Chen, Ben Liao, Zhe Wang, Chao Shen, Dongsheng Cao, Jian Wu, and Tingjun Hou. Could graph neural networks learn better molecular representation for drug discovery? a comparison study of descriptor-based and graph-based models. *Journal of cheminformatics*, 13:1–23, 2021.
- Weiwei Jiang and Jiayun Luo. Graph neural network for traffic forecasting: A survey. *Expert systems with applications*, 207:117921, 2022.
- Wei Jin, Xianfeng Tang, Haoming Jiang, Zheng Li, Danqing Zhang, Jiliang Tang, and Bin Ying. Condensing graphs via one-step gradient matching. *Proceedings of the 28th ACM SIGKDD Conference on Knowledge Discovery and Data Mining*, 2022a. URL <https://api.semanticscholar.org/CorpusID:249712265>.
- Wei Jin, Lingxiao Zhao, Shichang Zhang, Yozen Liu, Jiliang Tang, and Neil Shah. Graph condensation for graph neural networks, 2022b. URL <https://arxiv.org/abs/2110.07580>.
- Thomas N Kipf and Max Welling. Semi-supervised classification with graph convolutional networks. *arXiv preprint arXiv:1609.02907*, 2016.
- G. Li, Matthias Müller, Ali K. Thabet, and Bernard Ghanem. Deepgcns: Can gcns go as deep as cnns? *2019 IEEE/CVF International Conference on Computer Vision (ICCV)*, pp. 9266–9275, 2019. URL <https://api.semanticscholar.org/CorpusID:201070021>.
- Arthur Liberzon, Chet Birger, Helga Thorvaldsdóttir, Mahmoud Ghandi, Jill P Mesirov, and Pablo Tamayo. The molecular signatures database hallmark gene set collection. *Cell systems*, 1(6):417–425, 2015.
- Mengyang Liu, Shanchuan Li, Xinshi Chen, and Le Song. Graph condensation via receptive field distribution matching, 2022. URL <https://arxiv.org/abs/2206.13697>.
- Yilun Liu, Ruihong Qiu, and Zi Huang. Cat: Balanced continual graph learning with graph condensation. In *2023 IEEE International Conference on Data Mining (ICDM)*, pp. 1157–1162. IEEE, 2023.
- Andreas Loukas. Graph reduction by local variation. *ArXiv*, abs/1808.10650, 2018. URL <https://api.semanticscholar.org/CorpusID:52144738>.
- Kelong Mao, Jieming Zhu, Xi Xiao, Biao Lu, Zhaowei Wang, and Xiuqiang He. Ultragen: ultra simplification of graph convolutional networks for recommendation. In *Proceedings of the 30th ACM international conference on information & knowledge management*, pp. 1253–1262, 2021.
- Joseph J Pfeiffer III, Sebastian Moreno, Timothy La Fond, Jennifer Neville, and Brian Gallagher. Attributed graph models: Modeling network structure with correlated attributes. In *Proceedings of the 23rd international conference on World wide web*, pp. 831–842, 2014.
- Janet Piñero, Juan Manuel Ramírez-Anguita, Josep Saüch-Pitarch, Francesco Ronzano, Emilio Centeno, Ferran Sanz, and Laura I Furlong. The disgenet knowledge platform for disease genomics: 2019 update. *Nucleic acids research*, 48(D1):D845–D855, 2020.
- Jesse Read, Bernhard Pfahringer, Geoff Holmes, and Eibe Frank. Classifier chains for multi-label classification. *Machine learning*, 85:333–359, 2011.
- Luana Ruiz, Luiz Chamon, and Alejandro Ribeiro. Graphon neural networks and the transferability of graph neural networks. *Advances in Neural Information Processing Systems*, 33:1702–1712, 2020.
- Ozan Sener and Silvio Savarese. Active learning for convolutional neural networks: A core-set approach. *arXiv preprint arXiv:1708.00489*, 2017.
- Cosma Rohilla Shalizi and Andrew C Thomas. Homophily and contagion are generically confounded in observational social network studies. *Sociological methods & research*, 40(2):211–239, 2011.
- Min Shi, Yufei Tang, and Xingquan Zhu. Mlne: Multi-label network embedding. *IEEE transactions on neural networks and learning systems*, 31(9):3682–3695, 2019.

- 
- Min Shi, Yufei Tang, Xingquan Zhu, and Jianxun Liu. Multi-label graph convolutional network representation learning. *IEEE Transactions on Big Data*, 8(5):1169–1181, 2020.
- Jianheng Tang, Jiajin Li, Ziqi Gao, and Jia Li. Rethinking graph neural networks for anomaly detection. In *International Conference on Machine Learning*, pp. 21076–21089. PMLR, 2022.
- Grigorios Tsoumakas and Ioannis Katakis. Multi-label classification: An overview. *Data Warehousing and Mining: Concepts, Methodologies, Tools, and Applications*, pp. 64–74, 2008.
- Petar Velickovic, Guillem Cucurull, Arantxa Casanova, Adriana Romero, Pietro Lio, Yoshua Bengio, et al. Graph attention networks. *stat*, 1050(20):10–48550, 2017.
- Jianian Wang, Sheng Zhang, Yanghua Xiao, and Rui Song. A review on graph neural network methods in financial applications. *arXiv preprint arXiv:2111.15367*, 2021.
- Lin Wang, Wenqi Fan, Jiatong Li, Yao Ma, and Qing Li. Fast graph condensation with structure-based neural tangent kernel. In *Proceedings of the ACM on Web Conference 2024*, pp. 4439–4448, 2024.
- Tongzhou Wang, Jun-Yan Zhu, Antonio Torralba, and Alexei A Efros. Dataset distillation. *arXiv preprint arXiv:1811.10959*, 2018.
- Max Welling. Herding dynamical weights to learn. In *Proceedings of the 26th annual international conference on machine learning*, pp. 1121–1128, 2009.
- Shiwen Wu, Fei Sun, Wentao Zhang, Xu Xie, and Bin Cui. Graph neural networks in recommender systems: a survey. *ACM Computing Surveys*, 55(5):1–37, 2022.
- Zonghan Wu, Shirui Pan, Fengwen Chen, Guodong Long, Chengqi Zhang, and S Yu Philip. A comprehensive survey on graph neural networks. *IEEE transactions on neural networks and learning systems*, 32(1):4–24, 2020.
- Xinyue Xia, Gal Mishne, and Yusu Wang. Implicit graphon neural representation. In *International Conference on Artificial Intelligence and Statistics*, pp. 10619–10634. PMLR, 2023.
- Shunxin Xiao, Shiping Wang, Yuanfei Dai, and Wenzhong Guo. Graph neural networks in node classification: survey and evaluation. *Machine Vision and Applications*, 33(1):4, 2022.
- Hongjia Xu, Liangliang Zhang, Yao Ma, Sheng Zhou, Zhuonan Zheng, and Bu Jiajun. A survey on graph condensation. *arXiv preprint arXiv:2402.02000*, 2024.
- Keyulu Xu, Weihua Hu, Jure Leskovec, and Stefanie Jegelka. How powerful are graph neural networks? *arXiv preprint arXiv:1810.00826*, 2018.
- Zhe Xu, Yuzhong Chen, Menghai Pan, Huiyuan Chen, Mahashweta Das, Hao Yang, and Hanghang Tong. Kernel ridge regression-based graph dataset distillation. In *Proceedings of the 29th ACM SIGKDD Conference on Knowledge Discovery and Data Mining*, pp. 2850–2861, 2023.
- Beining Yang, Kai Wang, Qingyun Sun, Cheng Ji, Xingcheng Fu, Hao Tang, Yang You, and Jianxin Li. Does graph distillation see like vision dataset counterpart?, 2023. URL <https://arxiv.org/abs/2310.09192>.
- Xiaodi Yang, Shiping Yang, Qinmengge Li, Stefan Wuchty, and Ziding Zhang. Prediction of human-virus protein-protein interactions through a sequence embedding-based machine learning method. *Computational and structural biotechnology journal*, 18:153–161, 2020.
- Hanqing Zeng, Hongkuan Zhou, Ajitesh Srivastava, Rajgopal Kannan, and Viktor Prasanna. Graphsaint: Graph sampling based inductive learning method. *arXiv preprint arXiv:1907.04931*, 2019.
- Jiani Zhang, Xingjian Shi, Shenglin Zhao, and Irwin King. Star-gcn: Stacked and reconstructed graph convolutional networks for recommender systems. *arXiv preprint arXiv:1905.13129*, 2019a.

- 
- Muhan Zhang, Zhicheng Cui, Marion Neumann, and Yixin Chen. An end-to-end deep learning architecture for graph classification. In *Proceedings of the AAAI conference on artificial intelligence*, volume 32, 2018.
- Shichang Zhang, Atefeh Sohrabizadeh, Cheng Wan, Zijie Huang, Ziniu Hu, Yewen Wang, Jason Cong, Yizhou Sun, et al. A survey on graph neural network acceleration: Algorithms, systems, and customized hardware. *arXiv preprint arXiv:2306.14052*, 2023.
- Si Zhang, Hanghang Tong, Jiejun Xu, and Ross Maciejewski. Graph convolutional networks: a comprehensive review. *Computational Social Networks*, 6(1):1–23, 2019b.
- Xiao-Meng Zhang, Li Liang, Lin Liu, and Ming-Jing Tang. Graph neural networks and their current applications in bioinformatics. *Frontiers in genetics*, 12:690049, 2021.
- Yuchen Zhang, Tianle Zhang, Kai Wang, Ziyao Guo, Yuxuan Liang, Xavier Bresson, Wei Jin, and Yang You. Navigating complexity: Toward lossless graph condensation via expanding window matching. *arXiv preprint arXiv:2402.05011*, 2024.
- Bo Zhao and Hakan Bilen. Dataset condensation with distribution matching. In *Proceedings of the IEEE/CVF Winter Conference on Applications of Computer Vision*, pp. 6514–6523, 2023.
- Tianqi Zhao, Ngan Thi Dong, Alan Hanjalic, and Megha Khosla. Multi-label node classification on graph-structured data. *arXiv preprint arXiv:2304.10398*, 2023.
- Xin Zheng, Miao Zhang, Chunyang Chen, Quoc Viet Hung Nguyen, Xingquan Zhu, and Shirui Pan. Structure-free graph condensation: From large-scale graphs to condensed graph-free data. *Advances in Neural Information Processing Systems*, 36, 2024.
- Jie Zhou, Ganqu Cui, Shengding Hu, Zhengyan Zhang, Cheng Yang, Zhiyuan Liu, Lifeng Wang, Changcheng Li, and Maosong Sun. Graph neural networks: A review of methods and applications. *AI open*, 1:57–81, 2020.
- Yanqiao Zhu, Weizhi Xu, Jinghao Zhang, Yuanqi Du, Jieyu Zhang, Qiang Liu, Carl Yang, and Shu Wu. A survey on graph structure learning: Progress and opportunities. *arXiv preprint arXiv:2103.03036*, 2021.

## A Appendix

### A.1 Adapted GCond Algorithm

### A.2 Visualization of Multi-Label Datasets

In this section, we delve deeper into the characteristics of the condensed graphs by analyzing class distribution and label correlation within the multi-label datasets. This detailed examination is crucial for understanding how effectively the condensation methods preserve the multi-label relationships present in the original datasets.

After obtaining the full benchmark results, we provide a detailed analysis of the condensed graphs by examining the class distribution and label correlation within the synthetic graphs. These statistical properties are crucial for understanding how well the condensed graphs preserve the multi-label relationships present in the original datasets.

- **Label Correlation:** To analyze the relationships between labels in the dataset, we define the correlation matrix: Let  $G_{\text{labels}}$  be the set of labels from the original dataset  $\mathcal{G}$ , and  $Y$  be the corresponding original label matrix. We denote  $M(i, j)$  as the occurrence times of labels  $L_i$  and  $L_j$ , and  $N_i$  as the total number of times label  $L_i$  appears.

The conditional probability  $P(i, j)$  is defined as:

$$P(i, j) = \frac{M(i, j)}{N_i} \quad (24)$$

---

**Algorithm 1: Multi-Label GCond Adaptation**

---

**Input:** Training data  $\mathcal{G} = (A, X, Y)$

```
1 Initialize multi-label synthetic graph  $\mathcal{S}$  with  $X', Y'$ 
2 for  $k = 0$  to  $K - 1$  do
3   Initialize  $\theta_0 \sim P_{\theta_0}$ 
4   for  $t = 0$  to  $T - 1$  do
5      $D' \leftarrow 0$ 
6     Compute  $A' = g_\phi(X')$ , then  $\mathcal{S} = (A', X', Y')$ 
7     Compute  $\mathcal{L}^{\mathcal{G}} = \mathcal{L}(GNN_{\theta_t^{\mathcal{G}}}(A, X), Y)$ 
8     Compute  $\mathcal{L}^{\mathcal{S}} = \mathcal{L}(GNN_{\theta_t^{\mathcal{S}}}(A', X', Y'))$ 
9      $D' \leftarrow D' + D(\nabla_{\theta_t} \mathcal{L}^{\mathcal{G}}, \nabla_{\theta_t} \mathcal{L}^{\mathcal{S}})$ 
10    if  $t\%(\tau_1 + \tau_2) < \tau_1$  then
11      Update  $X' \leftarrow X' - \eta_1 \nabla_{X'} D'$ 
12    else
13      Update  $\phi \leftarrow \phi - \eta_2 \nabla_{\phi} D'$ 
14    Update  $\theta_{t+1} \leftarrow \text{opt}_{\theta}(\theta_t, \mathcal{S}, \tau_{\theta})$ 
15    Compute new adjacency matrix:  $A' = g_\phi(X')$ 
16    for each edge  $(i, j)$  in  $A'$  do
17      Update  $A'_{i,j} \leftarrow A'_{i,j}$  if  $A'_{i,j} > \delta$ , otherwise  $A'_{i,j} \leftarrow 0$ 
18 return  $(A', X', Y')$ 
```

---

This conditional probability matrix  $P$  models the edges as a co-occurrence matrix.

Next, we define the diagonal matrix  $D$  as follows:

$$D = \text{Diag}(P) \quad (25)$$

Finally, the Laplacian matrix  $L_o$  is computed as:

$$L_o = D - P \quad (26)$$

By computing the label correlation matrix, we investigate whether the co-occurrence patterns between labels in the original graph are retained in the condensed graph.

- **Class Distribution:** We analyze how evenly or unevenly the labels are distributed across the classes in different datasets by index, which helps assess the quality of the condensation process.

Following the above definition, we report the visualizations of different datasets as follows. The label correlation and class distribution are shown in Figures 2 and 3, respectively. We find that the more complex the labels, the more the condensation methods would rely on structure and become more random. For future work, more suitable methods need to be fit to multi-label scenarios.

### A.3 F1-Macro Results of Adaptation

Figures 4, 5 and 6 show the visualizations of different adaptation strategies measured by F1-micro score. To further investigate the effectiveness of the methods, we also report the F1-macro score in Tables 6, 7 and 8.

### A.4 Class-Weighted Optimization

Let  $N_{\max} = \max_{c \in \{0, \dots, C-1\}} N_c$  is the maximum number of samples across all classes. For each class  $c$  the class-wise coefficient is defined as:

$$\alpha_c = \frac{N_c}{N_{\max}} \quad (27)$$

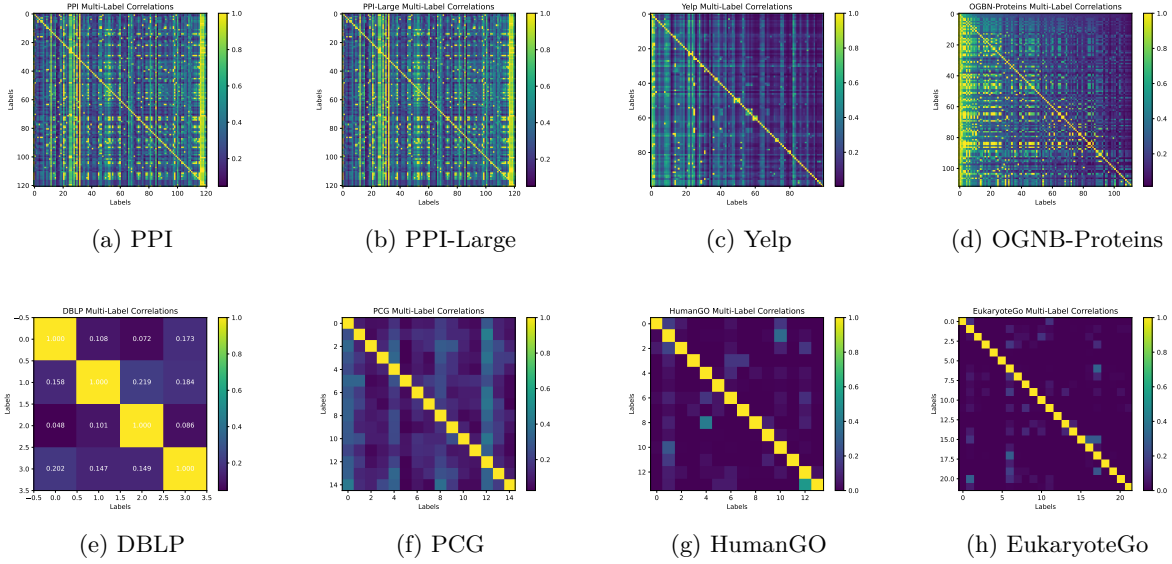


Figure 2: Multi-label Correlation Visualization

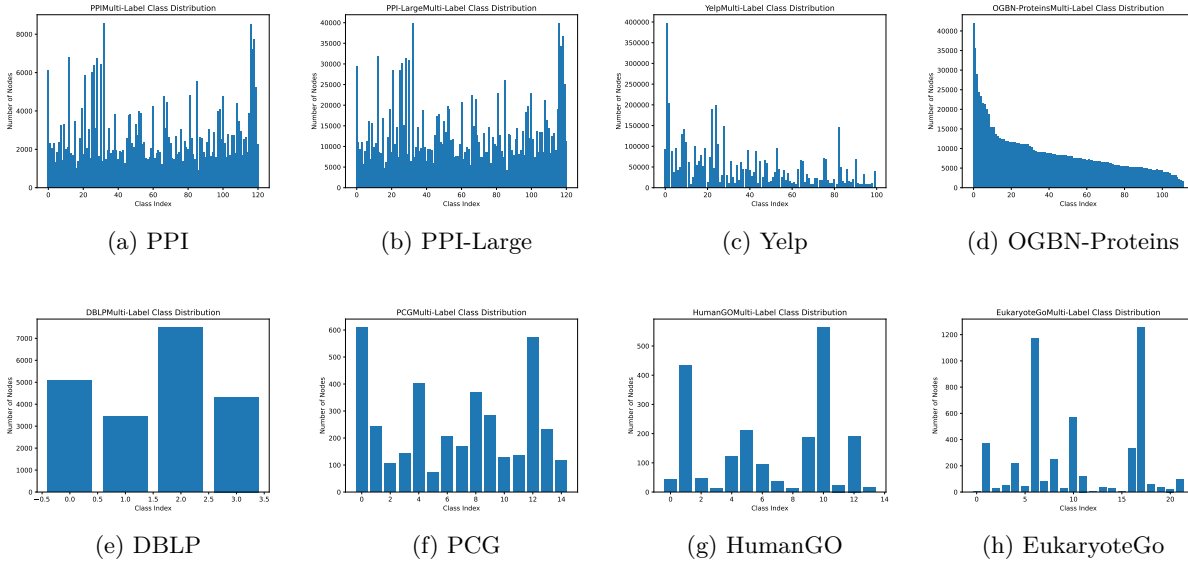


Figure 3: Multi-label Class Distribution Visualization

The total loss for all the  $N$  nodes would be the sum over all the classes and their respective nodes  $N_c$ :

$$\mathcal{L}_{single-label} = \sum_{c=0}^{C-1} \alpha_c \sum_{j \in N_c} \ell_{CE}(z_j, y_j) \quad (28)$$

This is the general equation for different methods, as the condensation part is using the  $\mathcal{M}(\cdot)$  as the matching loss, for example, GCond would compute the gradient for each class with class-wise coefficient and sum them up to get the final loss.

Furthermore, for each task we are working on the binary classification problem. To better capture the contribution of each class in multi-label, we introduce class weights  $\omega \in \mathbb{R}^K$  for each task  $k$ :

$$\ell_{BCE}(z_{j,k}, y_{j,k}) = -\omega_k (y_{j,k} \log(\sigma(z_{j,k})) + (1 - y_{j,k}) \log(\sigma(z_{j,k}))), \quad (29)$$

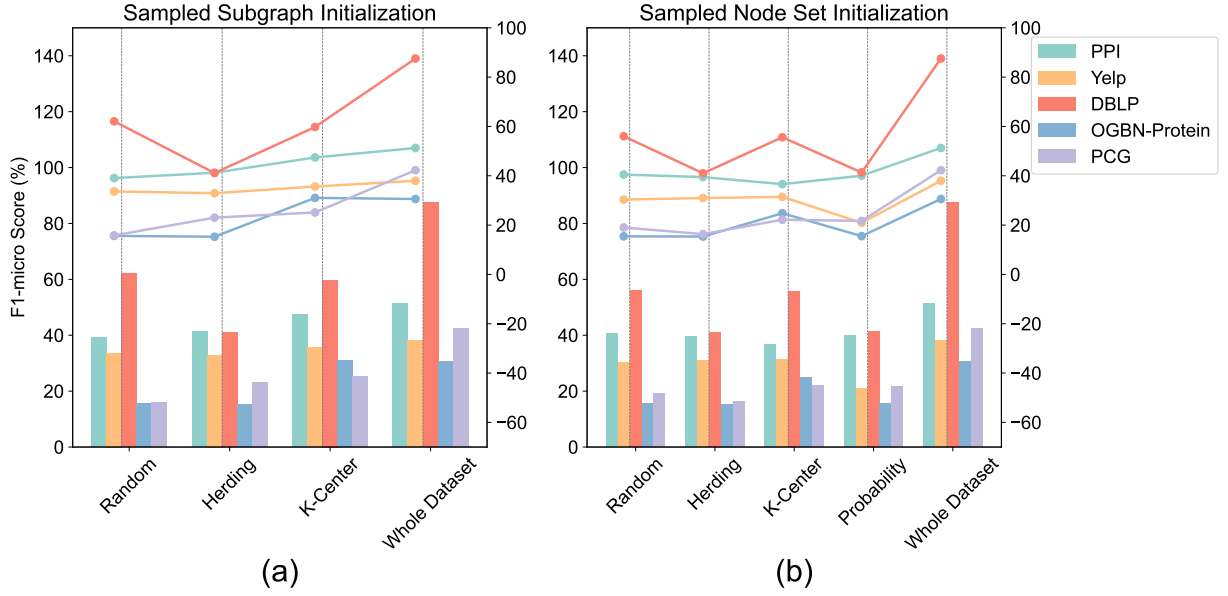


Figure 4: Different Initialization Methods Performance. Performance metrics of the model, with the F1-score represented as a decimal value.

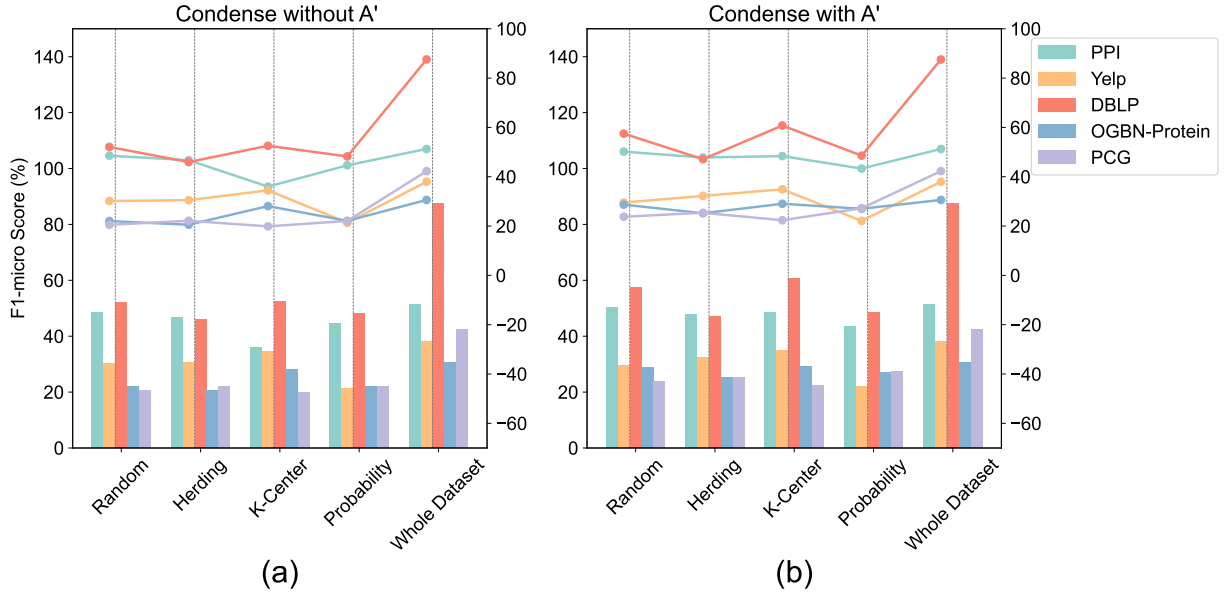


Figure 5: Performance Optimized by SoftMargin Loss. Performance metrics of the model, with the F1-score represented as a decimal value.

where  $\omega_k$  is the positive class weight, scaling the loss for each positive class  $y_{i,k} = 1$ . Therefore, the final loss of multi-label classification is:

$$\mathcal{L}_{multi-label} = -\frac{1}{N} \sum_{j=0}^{N-1} \sum_{k=0}^{K-1} \omega_k (y_{j,k} \log(\sigma(z_{j,k})) + (1 - y_{j,k}) \log(1 - \sigma(z_{j,k}))) \quad (30)$$

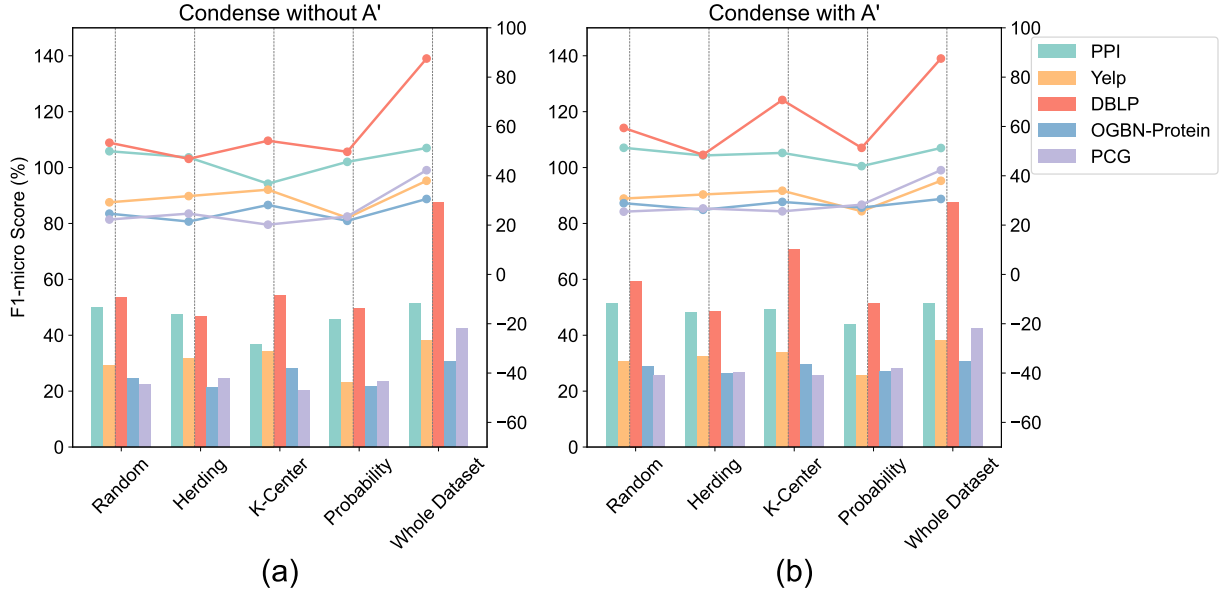


Figure 6: Performance Optimized by BCE Loss. Performance metrics of the model, with the F1-score represented as a decimal value.

Datasets	C-rate	Random		Herding		K-Center		Probability	Whole Dataset
		Subgraph	Nodes	Subgraph	Nodes	Subgraph	Nodes		
PPI	1.00%	12.58	10.67	11.66	17.98	17.36	<b>18.37</b>	12.55	30.06
Yelp	0.02%	5.09	3.76	5.64	3.66	<b>12.30</b>	8.78	2.87	15.18
DBLP	0.80%	56.00	51.43	15.63	15.41	<b>56.90</b>	52.74	15.68	86.39
OGBN-Pro	0.1%	2.12	7.12	5.21	7.17	<b>10.13</b>	6.42	6.36	9.16
PCG	4%	5.20	9.69	<b>13.84</b>	6.45	5.73	7.10	11.35	31.49

Table 6: F1 Macro Score(%) of Coreset Method with Different Initialization Strategies

This is helpful when there is an imbalance between the number of positive and negative samples. The F1-micro results are shown in Table 9 and Figure 7. F1-macro results are shown in Table 10.

Datasets	C-rate	Random		Herding		K-Center		Probability		Whole Dataset
		Without $A'$	With $A'$	Without $A'$	With $A'$	Without $A'$	With $A'$	Without $A'$	With $A'$	
PPI	1.00%	22.60	28.33	<b>30.37</b>	18.32	11.62	23.12	16.66	12.61	30.06
Yelp	0.02%	3.72	6.98	3.57	3.99	6.37	<b>9.02</b>	2.13	1.86	15.18
DBLP	1%	35.81	37.84	27.08	27.11	32.21	<b>49.36</b>	42.33	38.08	86.39
OGBN-Pro	0.10%	4.36	5.47	5.37	<b>7.18</b>	5.26	5.32	3.21	4.76	9.16
PCG	4%	12.42	13.86	10.09	<b>15.50</b>	7.34	9.47	13.29	6.50	31.49

Table 7: F1-Macro Score (%) of GCond Method with Random/Herding/K-Center/Probability Distribution Initialization with/without Learning from Graph Structure for SoftMarginLoss

Datasets	C-rate	Random		Herding		K-Center		Probability		Whole Dataset
		Without $A'$	With $A'$	Without $A'$	With $A'$	Without $A'$	With $A'$	Without $A'$	With $A'$	
PPI	1.00%	22.82	<b>23.86</b>	21.72	21.35	20.69	21.47	17.68	20.62	30.06
Yelp	0.02%	3.57	<b>8.02</b>	4.24	4.13	6.13	6.22	4.00	3.07	15.18
DBLP	1%	34.89	51.44	26.94	28.28	34.87	<b>68.44</b>	38.36	39.87	86.39
OGBN-Pro	0.10%	6.79	6.19	5.87	7.30	4.98	<b>7.47</b>	2.89	4.99	9.16
PCG	4%	7.83	7.29	<b>15.17</b>	14.27	8.02	13.32	13.13	11.30	31.49

Table 8: F1-Macro Score (%) of GCond Method with Random/Herding/K-Center/Probability Distribution Initialization with/without Learning from Adjacent Nodes for BCELoss

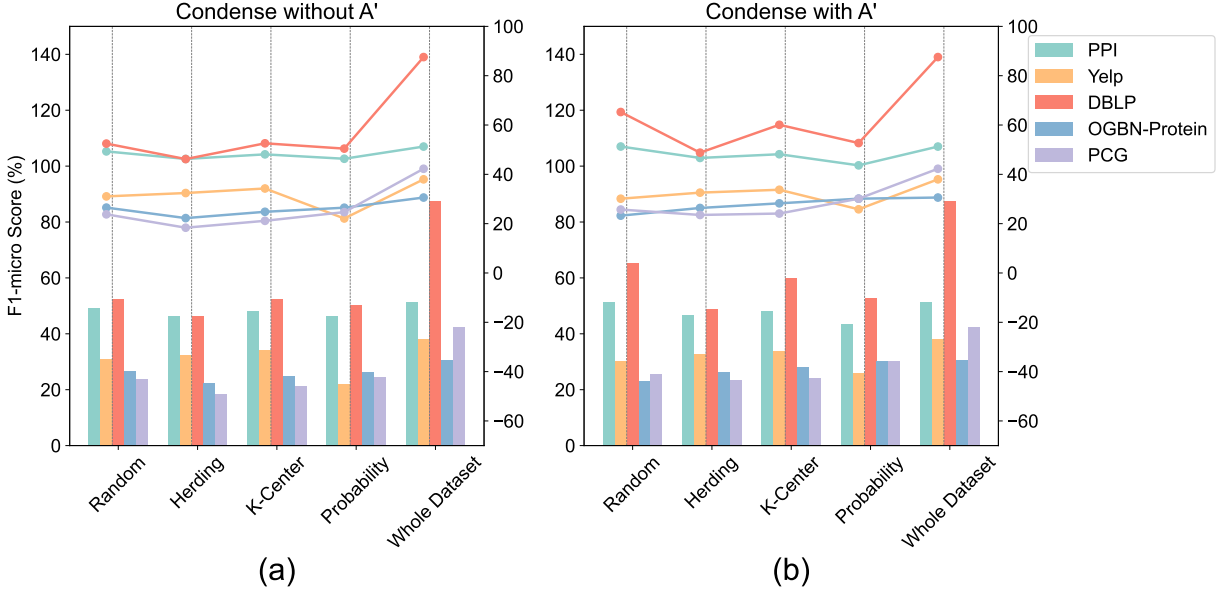


Figure 7: Performance Optimized by BCE Loss with Class Weight  $\omega$

Datasets	C-rate	Random		Herding		K-Center		Probability		Whole Dataset
		Without $A'$	With $A'$	Without $A'$	With $A'$	Without $A'$	With $A'$	Without $A'$	With $A'$	
PPI	1.00%	49.30	<b>51.28</b>	46.25	46.65	48.10	48.15	46.32	43.64	51.26
Yelp	0.02%	31.06	30.12	32.42	32.58	<b>34.26</b>	33.75	22.10	25.82	37.97
DBLP	0.80%	52.47	<b>65.27</b>	46.19	48.79	52.58	60.09	50.43	52.69	87.55
OGBN-Proteins	0.10%	26.51	23.25	22.25	26.36	24.81	28.24	26.47	<b>30.13</b>	30.59
PCG	4%	23.78	25.72	18.36	23.53	21.15	24.10	24.68	<b>30.13</b>	42.26

Table 9: F1-Micro Score (%) of GCond Method with Random/Herding/K-Center/Probability Distribution Initialization with/without Learning from Adjacent Nodes for BCE Loss and Balanced Coefficient

Datasets	C-rate	Random		Herding		K-Center		Probability		Whole Dataset
		Without $A'$	With $A'$	Without $A'$	With $A'$	Without $A'$	With $A'$	Without $A'$	With $A'$	
PPI	1.00%	21.75	25.65	15.55	27.21	27.09	<b>31.97</b>	14.31	21.43	30.06
Yelp	0.02%	3.91	6.49	4.06	5.16	<b>11.72</b>	7.78	1.86	2.42	15.18
DBLP	0.80%	32.79	<b>61.83</b>	26.44	29.25	32.64	56.29	37.78	42.11	86.39
OGBN-Pro	0.10%	4.60	6.05	3.54	4.69	6.42	7.89	4.38	<b>8.56</b>	9.16
PCG	4%	13.26	11.93	12.24	<b>15.75</b>	5.70	9.88	11.60	8.56	31.49

Table 10: F1-Macro Score (%) of GCond Method with Random/Herding/K-Center/Probability Distribution Initialization with/without Learning from Adjacent Nodes for BCE Loss and Balanced Coefficient